Supplementary Material

Supplementary Methods

Mouse care

Mice with the *Oatp1c1* knockout allele (MGI:5308446) were generated on a C57BL/6 background.[1] The *Mct8* knockout line (MGI:3710233) was backcrossed for more than 10 generations on a C57BL/6 background.[2] The local animal ethics committee (Ministerium für Energiewende, Landwirtschaft, Umwelt, Natur und Digitalisierung, Kiel, Germany) approved all animal experiments (11-1/17 and 97-9/19). Mice were kept at constant temperature (22 °C) under a 12-h light/dark cycle and fed *ad libitum* with standard laboratory chow (2.98 kcal g^{-1}; Altromin 1310M, Hannover, Germany) and water in individually ventilated cages. We enriched mouse cages with igloos (new-born) and nestlets. The sex of mice was balanced between experimental groups, details are provided in Supplementary Table 1.

Generation of AAV-BR1-*Mct8* vector

RNA was isolated from a C57BL/6 mouse whole-brain lysate using the RNAeasy kit (Qiagen), followed by cDNA synthesis using the Omniscript RT kit (Qiagen) and oligo(dT) primer. *Mct8* mRNA (transcript variant 1) was amplified by PCR using GoTaq polymerase (Promega) and the primers "*Mct8*_EcoRI_fw": 5'-GAT CGA ATT CGC CAC CAT GGC GCT GCC AAG CCC GGC-3' and "Mct8_BsrGI_rev": 5'-GAT CTG TAC ATT AAA TGG GCT CTT CAG GTG TTG GG-3'. The *Mct8* amplicon was used to replace the transgene insert of the plasmid pAAV-CAG-BMP2-2A-Venus (provided by Dr. R. Sprengel, MPI Heidelberg, Germany) by digestion with EcoRI and BsrGI and the whole ligated pAAV transgene cassette, including AAV2 ITRs, CAG promoter, *Mct8* ORF, WPRE and the bGH polyadenylation signal was transferred into the pFastBac1 plasmid (Thermo Fisher). AAV-BR1-*Mct8* viral vector was produced in Sf9 insect cells using the modified baculovirus expression system.[3,4] Sf9 insect cells were cultured in Insect X-Press medium (Lonza, Basel, Switzerland) containing 10 mg/l gentamicin (Sigma, Darmstadt, Germany) and infected with high-titre stocks of two recombinant baculoviruses, one of which contained the AAV2-NRGTEWD ("AAV-BR1") rep and cap

genes and the other one the aforementioned CAG promoter-driven *Mct8* expression cassette.[5] Cells were cultured at 27 °C and 110 rpm. AAV-BR1-*Mct8* vector was purified by ultracentrifugation in a discontinuous iodixanol gradient, according to a previously published protocol.[6] After ultracentrifugation, AAVs in the 40% iodixanol fraction were aspirated and transferred to 10,000 MWCO Vivaspin tubes (Sartorius, Göttingen, Germany) for dialysis in PBS. The production of AAV-BR1-*Gfp* has been described previously.[7]

Intravenous injection of AAV-BR1-*Mct8*

For the treatment of neonatal mice with AAV-BR1 vectors, the dam was removed to a separate cage while intravenously injecting AAV-BR1-*Mct8* or AAV-BR1-*Gfp* ($1*10^{12}$ gp in 50 µl) in new-born pups using insulin syringes and 30-G cannulas. They were anesthetized by placing them on wet ice for 30-50 seconds. Under a stereomicroscope, vectors were injected into the temporal facial vein. After the injection, the needle was left within the vein for an additional 10-15 seconds to prevent backflow of the injected solution. After 2-3 minutes, pups were returned to the home cage and gently covered with bedding to ensure that the dam accepted the pups. At P30, AAV-BR1-*Mct8* ($4.5*10^{12}$ gp in 75 µl) was injected in the lateral tail vein, using 1-ml syringes and 30-G cannulas.

Immunofluorescence staining and image quantification

Mice were transcardially perfused with phosphate-buffered saline (PBS) plus 4% paraformaldehyde (PFA) or with PBS only. Brains were removed, post-fixed in 4% PFA prepared in PBS for 24 hours at 4 °C; then, the tissues were rinsed three times with PBS. The forebrain was sectioned coronally and the cerebellum sagittally, both at a thickness of 45 µm. Brain sections were rinsed with PBS three times and permeabilized with 0.2% Triton X-100 (in PBS) for 20 minutes. After the brain sections were incubated for 1 hour with 5% bovine serum albumin, the following antibodies were added for 12 hours: rabbit anti-parvalbumin (1:2,000, Swant PV), rabbit anti-calbindin (1:1,000, Cell Signaling Technology 2136), rabbit anti-MCT8 (1:1,000, Sigma HPA003353), rat anti-myelin basic protein (1:1,000, Millipore

MAB386), rabbit anti-Olig2 (1:500, Sigma-Aldrich AB9619), mouse anti-α-tubulin (1:2,000, Sigma-Aldrich T9026), chicken anti-vimentin (1:400, Sigma-Aldrich AB5733), mouse anti-APC (CC-1, 1:100, Abcam AB16794), mouse anti-NeuN (1:1,000, Millipore MAB377), mouse anti-GAD67 (1:1,000, Millipore MAB5406), rat anti-CD31 (1:500, BioRad MCA2388), goat anti-collagen IV (1:200, BioRad 134001). Sections were washed in PBS three times and incubated in the following secondary antibodies: donkey anti-rat IgG Alexa fluor-488 (1:200, ThermoFisher A-21208), donkey anti-goat IgG Alexa fluor-555 (1:200, Invitrogen A-21432), donkey anti-rabbit IgG Alexa fluor-555 (1:500, Invitrogen A-31572), donkey anti-rabbit IgG Alexa fluor-488 (1:500, Invitrogen A21206), donkey anti-mouse IgG Alexa fluor-555 (1:500, Invitrogen A-21432), donkey anti-rat IgG Alexa fluor-647 (1:500, Abcam ab150155), donkey anti-goat IgG Cy3 (1:500, Jackson ImmunoResearch 705-165-147), and donkey anti-mouse IgG Alexa fluor-647 (1:600, ThermoFisher A-31571). After washing in PBS, sections were incubated in DAPI (1 μg/ml in PBS) for 10 minutes, washed again in PBS, mounted on precoated slides, and coverslipped using Dako Fluorescence mounting medium (S3023). For MCT8 immunofluorescence staining, brain samples were snap-frozen and sectioned at 20-μm thickness. Then, the brain sections were fixed using 100% ethanol for 10 seconds as published previously [8]. Images were captured using a fluorescence microscope (Leica DMI 6000B) or a confocal microscope (Leica TCS SP5) and analysed using the software LAS AF and ImageJ (NIH, 1.47v).

We stained myelin in 45-μm-thick coronal vibratome sections of the forebrain of P33 mice using the FluoroMyelin reagent (Thermo Fisher F34651) following the manufacturer's protocol. Briefly, sections were permeabilized in Triton X-100 (0.2% in PBS) for 30 minutes, stained with FluoroMyelin Green Dye (1:2,000) and DAPI and analysed with a fluorescence microscope.

We manually counted Olig2-positive cells in somatosensory cortex (1 mm^2) or corpus callosum (0.3 mm^2); CC1-positive cells in somatosensory cortex (0.75 mm^2); and parvalbumin-positive cells in the somatosensory cortex (2.5 mm^2). String vessels were counted manually in the cerebral cortex as described previously.[7] The lengths of string vessels were normalised to the total vessel length of the image. Fluorescence intensity of GAD67, MBP, FluoroMyelin, and IgG staining was quantified by using ImageJ as mean grey area. IgG intensity was measured outside of collagen IV-positive vessels. For image quantification, we used 2 – 6 sections per animal and presented the average.

In situ hybridization

cDNA fragments corresponding to mouse *Mct8* (nt 787-1222, Genbank accession number AF045692), *Nrgn* (nt 498–1005, Genbank accession number NM 022029.2), *Trh* (nt 202-733, Genbank accession number NM_009426.3), *Tshb* (nt 190-443, Genbank accession number M10902), *Dio2* (nt 131-1045 Genbank accession number NM_010050.2) and *Klf9* (nt 693-1227, Genbank accession number NM_010638.4) were generated by PCR and inserted into the pGEM-T Easy vector (Promega). The pCRII-TOPO system was used to insert cDNA fragments of *Hr* (nt 902-1598, Genbank accession number NM_021877.2) and *Aldh1a1* (nt 1380-1941, Genbank accession number NM_013467.3). P^{33}-conjugated UTP containing radiolabelled probes were synthesized by *in vitro* transcription (Hartmann Analytic, Braunschweig, Germany). Overall, the radiolabelled ISH procedure was performed as reported previously.[9]

Brain sections were fixed in PFA (4% in PBS, pH 7.4) for 1 hour and permeabilized in Triton-X (0.4% in PBS) for 20 minutes. Then, an acetylation step was performed using triethanolamine (0.1 M, pH 8.0, containing 0.25% (v/v) acetic anhydride). Sections were dehydrated and incubated with hybridization buffer (50% formamide, 10% dextran sulfate, 0.6 M NaCl, 10 mM Tris–HCl pH 7.5, 1× Denhardt's solution, 100 µg/ml sonicated salmon sperm DNA, 1 mM EDTA, and 0.5 mg/ml t-RNA) containing complementary P^{33}-labeled RNA probes for 12 hours at 58 °C in a humidified chamber. The radiolabelled *Trh* and *Tshb* RNA probes were diluted to a concentration of $1*10^4$ cpm/µl, and *Hr*, *Aldh1a1*, *Mct8*, *Klf9*, *Nrgn*, and *Dio2* RNA probes were diluted with a concentration of $2*10^4$ cpm/µl in hybridization buffer. After hybridization, the sections were rinsed with 2X sodium citrate saline (0.3 M NaCl, 0.03 M sodium citrate, pH 7.0) and were incubated in ribonuclease A/T1 (Sigma-Aldrich R1003-100 KU) at 37 °C for 30 minutes. Then, the sections were washed with 0.2X sodium citrate saline at 65 °C for 1 hour and dehydrated using 50% and 70% ethanol. Finally, the sections were dipped in NTB nuclear emulsion (Kodak), air dried overnight, and stored at 4 °C for 15 days (*Trh, Hr*), 10 days (*Tsh, Nrgn, Klf9*), or 12 days (*Mct8, Aldh1a1, Dio2*). Autoradiograms were developed and visualized under dark-field illumination.

Measurement of TH

On P21 mice were transcardially perfused with PBS and brain tissues were snap-frozen using dry ice. The levels of T3 and T4 in the brain tissue lysates were quantified according to the liquid chromatography-quadrupole time-of-flight mass spectrometry (LC-MS) method described previously. [10] Serum concentrations of total T3 and total T4 were determined by enzyme-linked immunosorbent assay (ELISA) (tT3: DNOVO53, NovaTec Immundiagnostica GmbH, Dietzenbach, Germany, detection limit 0.05 ng/mL, intra- and interassay variance <11%; tT4: ELISA, EIA-1781; DRG Instruments GmbH, Marburg, Germany, detection limit 0.5 ng/mL, intra- and interassay variance <4.5%).

Reverse transcription and real-time quantitative polymerase chain reaction

The total RNA was isolated from brain and liver samples using NucleoSpin® RNA columns (Macherey-Nagel) according to the manufacturer's instructions. Briefly, tissues were weighed (about 10 mg) and homogenized. The total RNA was adsorbed to the NucleoSpin® RNA column, washed with the recommended buffers and eluted with RNase-free H_2O (60 µl). Total RNA was quantified, and its purity was assessed using an UV-Vis spectrophotometer NanoDrop™ 2000c (Thermo Scientific). The RNA samples were stored at -80 °C. First-strand cDNA was synthesized from 300 ng up to 400 ng total RNA using M-MLV reverse transcriptase (Promega). cDNA was stored at -20 °C until quantitative PCR (qPCR) was performed with the LightCycler® 96 System (Roche). The following primers were used: *Dio1* fw, 5'-GCT GAA GCG GCT TGT GAT ATT-3', *Dio1* rev, 5'-GTT GTC AGG GGC GAA TCG G-3', amplicon length, 154 bp; *Gpd2* fw, 5'-GAA GGG GAC TAT TCT TGT GGG T-3', *Gpd2* rev, 5'-GGA TGT CAA ATT CGG GTG TGT-3', amplicon length 197 bp; *Hr* fw, 5'-GCG TCC ATA TGA CTG GCC TT-3', *Hr* rev, 5'-CCT TGT GGT AAA AGC CCT TGC-3', amplicon length 106 bp; *Aldh1a1* fw, 5'-CAG GAG TTT ACA TCA ACT GGG AGA-3', *Aldh1a1* rev, 5'-CCC AAA CTC CAA CCA AGA-3', amplicon length 118 bp; *Nrgn* fw, 5'-CCA CAT GGC GAG GAA GAA GAT A-3', *Nrgn* rev, 5'- TAA AAC GTT CAG CTC TGG CCT-3', amplicon length 119 bp; *Klf9* fw, 5'-GGA AAC

ACG CCT CCG AAA AG-3', *Klf9* rev, 5'-AAA GGG CCG TTC ACC TGT AT-3', amplicon length 116 bp; *Dio2* fw, 5'-TCC TAG ATG CCT ACA AAC AGG TTA-3', *Dio2* rev, 5'-CGG TCT TCT CCG AGG CAT AA-3', amplicon length 108 bp; *Ppia* fw, 5'-GCA TAC AGG TCC TGG CAT CT-3', *Ppia* rev, 5'-CAT CCA GCC ATT CAG TCT TGG -3', amplicon length 97 bp. For each primer, a master mix was prepared containing the Platinum SYBR Green qPCR SuperMix (Invitrogen). The reactions were performed in duplicate at a final volume of 25 µl per well according to the following protocol: pre-incubation, 10 minutes at 95 °C; amplification 30 seconds at 95 °C, 30 seconds at 60 °C and 30 seconds at 72 °C (40 cycles); melting, 10 seconds at 95 °C, 60 seconds at 65 °C and 1 seconds at 97 °C. Product purity was confirmed by dissociation curve and agarose gel analysis. Serial dilutions of known amounts of the cloned cDNA fragments of each gene were used to generate standard curves in a range of 10^3 to 10^8 copies.[11] Per sample, an amount of 12 or 16 ng RNA were used. Results were normalized to *Ppia* for each individual sample.

Immunoblotting

Immunoblotting was performed as described previously.[12] In brief, 20 µg brain protein were separated on 12% SDS polyacrylamide gels (TGX Stain Free Fast Cast, BioRad Laboratories), blotted on PVDF membrane (IPHV00010, Merck Millipore), probed with antibodies for PLP1 (1:1,000, Cell Signaling #E9V1N), MBP (1:1,000, Abcam ab218011) or Olig2 (1:1,000, Abcam ab109186) and visualized using Clarity Max ECL Substrate and the ChemiDoc system (BioRad Laboratories). Band intensity was quantified using ImageLab 6.1 (BioRad Laboratories) and normalized to total protein load.

Transduction of endothelial cells *in vitro*

Primary mouse brain endothelial cells from DKO and control with or without transduction with AAV-BR1-*Mct8* were cultured in 8-well chamber slides (Ibidi, cat. No. 80841) as described previously.[13] After removing the medium on day *in vitro* (DIV) 5, fresh DMEM medium (1 ml) containing viral particles ($5x10^9$ gp per well) was added. The plates were incubated at 37 °C and 5% CO_2 for 10 days without changing the medium. On DIV 15, we performed the T3 uptake assay. Parallel culture plates

were fixed with PFA (4%) for immunofluorescent staining. Briefly, cells were permeabilized with Triton X-100 (0.2% in PBS) for 20 minutes and incubated in primary antibodies against MCT8 and CD31 for 12 hours at 4 °C. Then, the cells were washed with PBS for three times and incubated with the following secondary antibodies: donkey anti-rabbit IgG Alexa fluor-555 and donkey anti-rat IgG Alexa fluor-488 and DAPI for 1 hour. Finally, the cells were washed with PBS for three times and the cover slips were mounted on glass slides using Dako Fluorescence mounting medium (S3023) for imaging using a fluorescence microscope.

T3 uptake assay

The T3 uptake assay is based on the Sandell-Kolthoff reaction and has been described previously,[14] but we adapted the method to 24-well plates. Cells were washed twice with PBS (0.5 ml per well). After adding uptake buffer (0.6 ml per well, containing 2 M NaCl, 2 M CaCl2, 0.6 M $MgCl_2$, 2.5 M KCl, 5 µM T3, and 5 µM silychristin (Sigma-Aldrich 51681-10MG, as indicated), the cells were incubated for 20 minutes at 37 °C and 5% CO_2. The uptake of T3 was stopped by removing the buffer, washing the cells twice with 0.1% BSA in PBS and once with ice-cold distilled water. Then, to release the iodide from T3 ammonium persulfate (0.2 ml, 0.6 M) was added to each well and the plates were incubated at 85 °C for 1 hour. After centrifugation for 1 minute at 900 *g*, 20 µl of supernatant was transferred into a black 96-well plate with clear bottom and filled up with distilled water to 50 µl. After adding 50 µl ceric solution (50 mM HEPES, 0.25 M $(NH_4)_4Ce(SO_4)_4$, 5M H_2SO_4) and 50 µl arsenous solution (2 M $NaAsO_2$, 5 M H_2SO_4, 2 M NaCl, 5.6 mM D-glucose) per well, the absorption was measured in a FLUOstar® Omega microplate reader (BMG LABTECH) at 405 nm every 60 seconds for 30 minutes.

Behaviour paradigms

Motor coordination was analysed with an accelerating Rotarod (Ugo Basile, 47600). Four-month-old male and female mice were familiarized to the system by allowing them to run once on the rotating rod with a constant velocity of 5 rpm for 300 seconds. On the following day, rod rotation was accelerated

from 5-50 rpm within the maximum testing period of 300 seconds. The animals were analysed on five consecutive days with two trials per day and the time the mice remained on the roller was monitored.

Beam walk testing was performed by training 4-month-old mice three times on three consecutive days. Animals were trained to cross a narrow beam to finally reach their home cage. In the experimental setup, a beam 100 cm in length and 10 mm on width was used. On three consecutive days, the animals were prompted to cross the beam three times. The time needed for each crossing and the total number of times the right and the left hind limbs slipped from the bar were recorded. We averaged the scores over all days of analysis.

Grip strength was measured with a high-precision force sensor (GSM, Ugo Basile, 47200). Four-month-old mice were placed with their forelimbs on the measuring wire. Then, mice were gently pulled backward and away from the wire with a uniform, straight draft. Recording was repeated five times per animal.

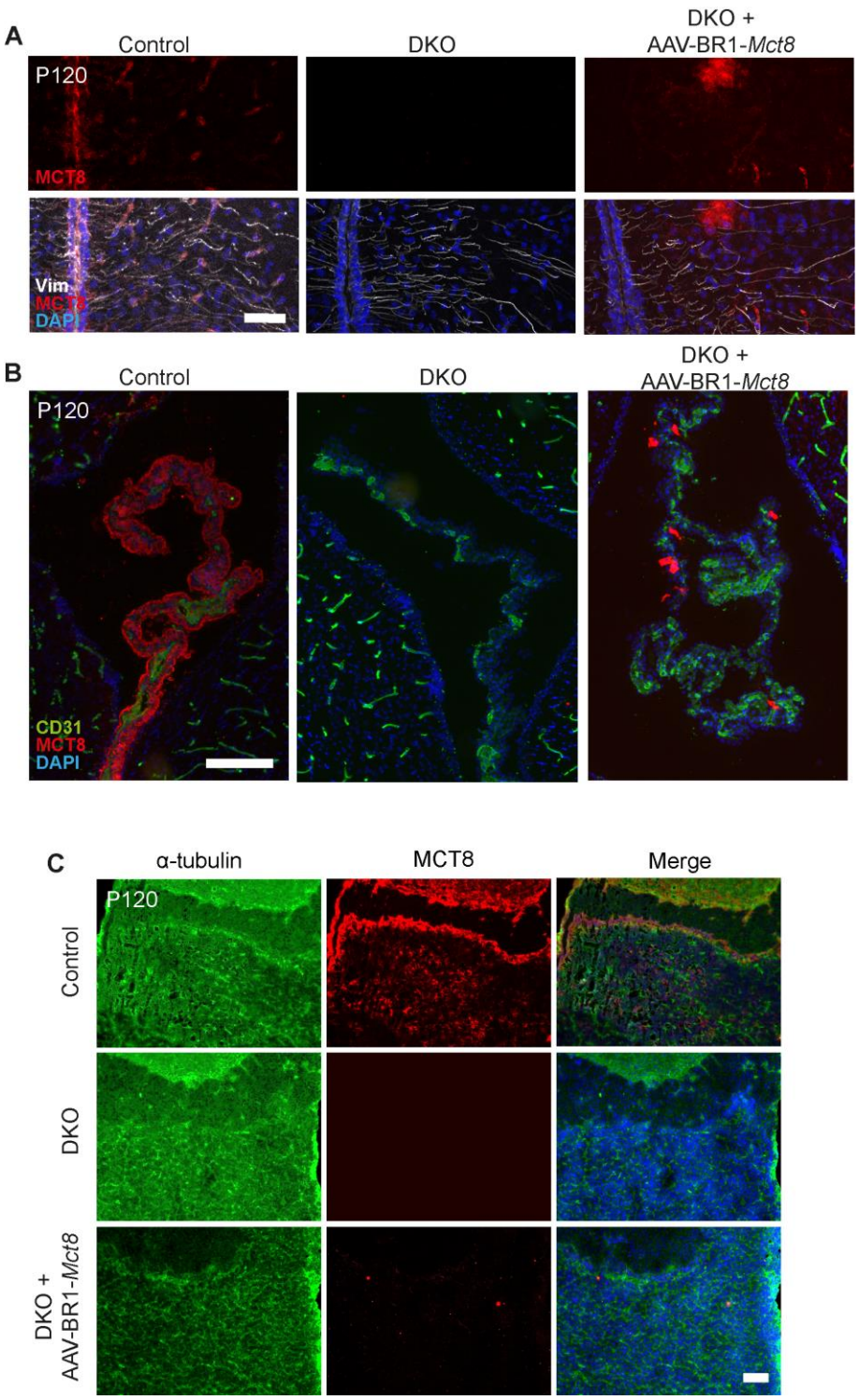

Supplementary Figure 1. MCT8 expression in brain and pituitary.

Brains and pituitary glands were collected from controls, DKO mice, and AAV-BR1-*Mct8*-treated DKO mice at P120. AAV-BR1-*Mct8* had been administered at P0. MCT8 and the cell specific markers vimentin (Vim, tanycytes; **A**), CD31 (endothelial cells; **B**) and α-tubulin (cytoskeleton; **C**) were detected by immunofluorescence staining. (**A**) In the mediobasal hypothalamus, vimentin-positive tanycytes of control mice expressed MCT8, whereas tanycytes in DKO mice with or without AAV-BR1-*Mct8* treatment showed no MCT8 expression. In the right panel, MCT8 expression in endothelial cells and in a cell with typical astrocytic morphology is visible. Scale bar, 50 µm. (**B**) Epithelial cells of the choroid plexus expressed MCT8 in control, but not in DKO mice. AAV-BR1-*Mct8* treatment transduced some scattered epithelial cells and no endothelial cells of the choroid plexus. Scale bar, 100 µm. (**C**) Pituitary

sections from control mice showed a strong immunofluorescence signal for MCT8, whereas sections from DKO with or without AAV-BR1-*Mct8* treatment showed no MCT8 expression. Scale bar, 100 µm.

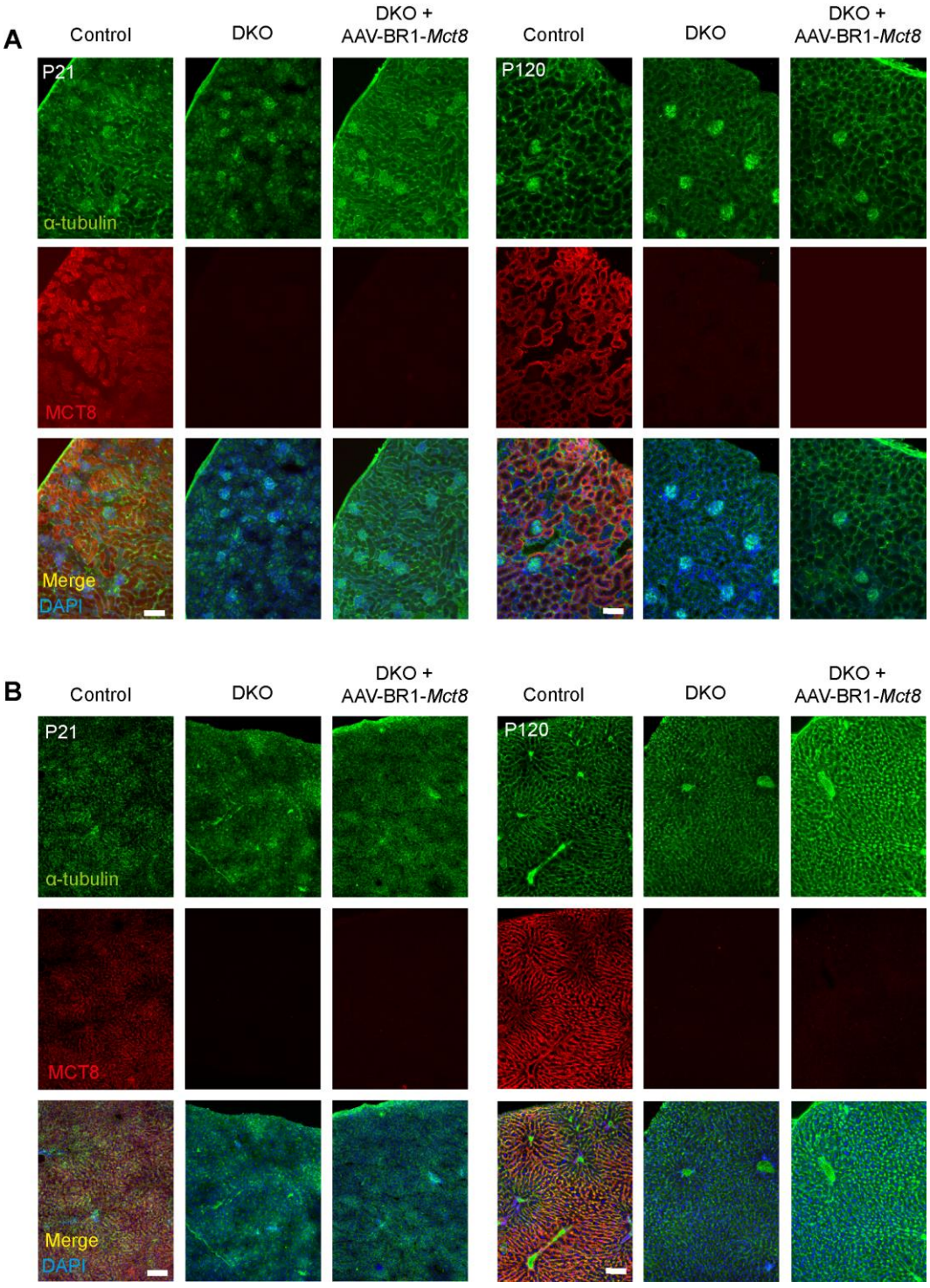

Supplementary Figure 2. MCT8 expression in peripheral tissues.

Kidney and liver tissues were collected from controls, DKO mice, and AAV-BR1-*Mct8*-treated DKO, mice at P21 (left) and P120 (right). AAV-BR1-*Mct8* had been administered at P0. MCT8 and the cell cytoskeleton marker α-tubulin were detected by immunofluorescence staining. (**A**) At P21 and P120, kidney sections showed a strong immunofluorescence signal for MCT8 in control animals but not in DKO mice with or without AAV-BR1-*Mct8* treatment. (**B**) At P21 and P120, liver sections showed a strong immunofluorescence signal for MCT8 in control mice but not in DKO animals with or without AAV-BR1-*Mct8* treatment. Scale bar, 100 µm.

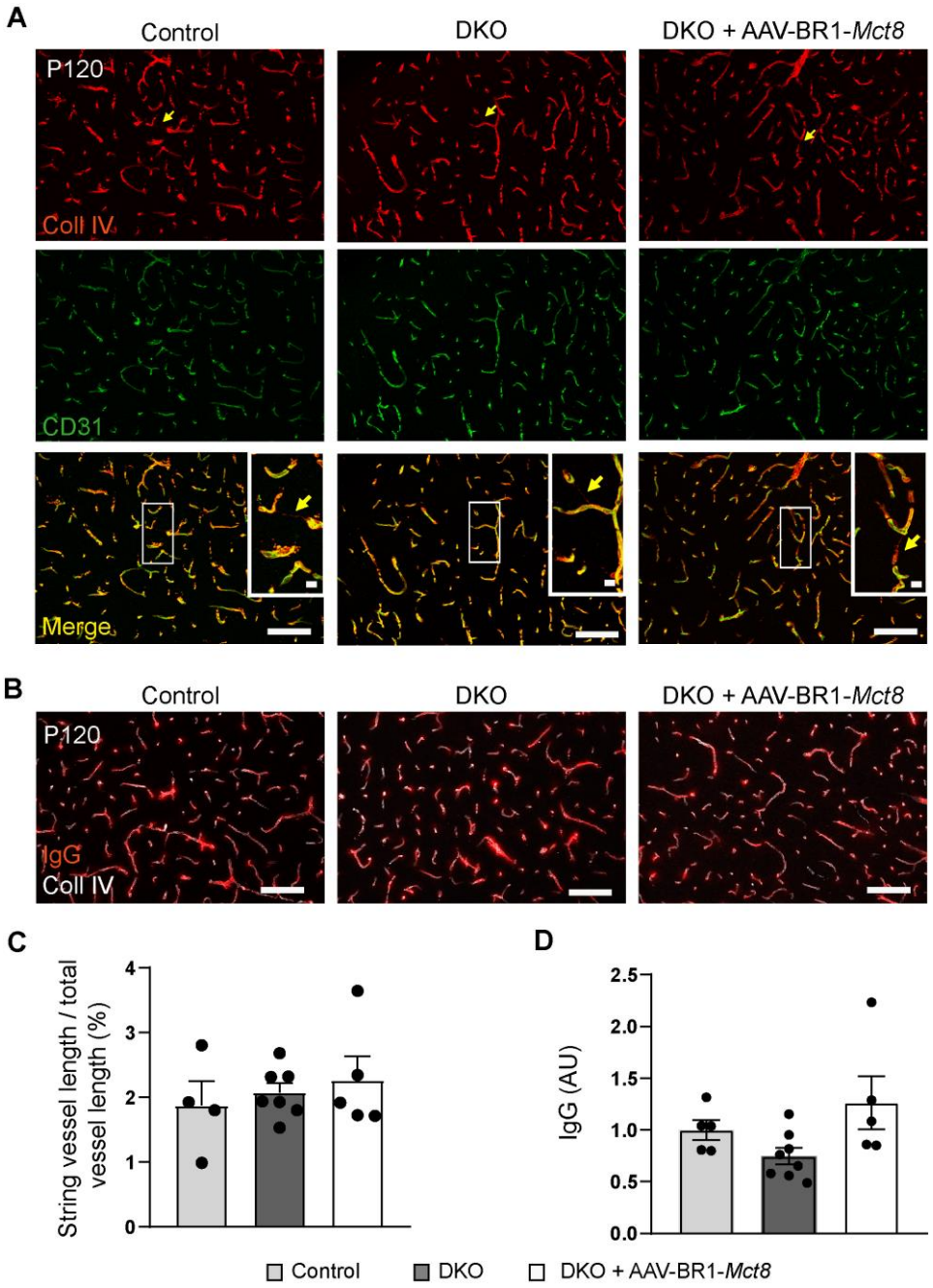

Supplementary Figure 3. Blood-brain barrier properties and string vessel length.

(**A**) To investigate whether transduction with AAV-BR1-*Mct8* impairs the viability of brain endothelial cells, cortical brain sections of P120 controls, DKO mice, and AAV-BR1-*Mct8*-treated DKO mice were stained for the endothelial marker CD31 and the basement membrane marker collagen IV. AAV-BR1-*Mct8* had been administered at P0. String vessels represent empty basement membrane tubes without inside CD31-positive endothelial cells and indicate endothelial cell loss (arrows). Insets, high magnifications of the boxed areas. Scale bars, 100 µm or 5 µm (insets). (**B**) To evaluate the tightness of the blood-brain barrier, IgG extravasation was measured outside of vessels. IgG was visualised in parallel to collagen IV (Coll IV). Scale bars, 100 µm. (**C**) Quantitative analyses of string vessels. We found no differences in string vessel length between control, DKO, and AAV-BR1-*Mct8*-treated DKO mice. One-way ANOVA, $F(2/13)=0.4268$, $P=0.6614$. (**D**) Quantification of IgG extravasation. We found no differences in parenchymal IgG between controls, DKO mice, and AAV-BR1-*Mct8*-treated DKO animals. One-way ANOVA, $F(2/15)=3.402$, $P=0.0605$. Each dot represents one animal. Means ± SEM are shown.

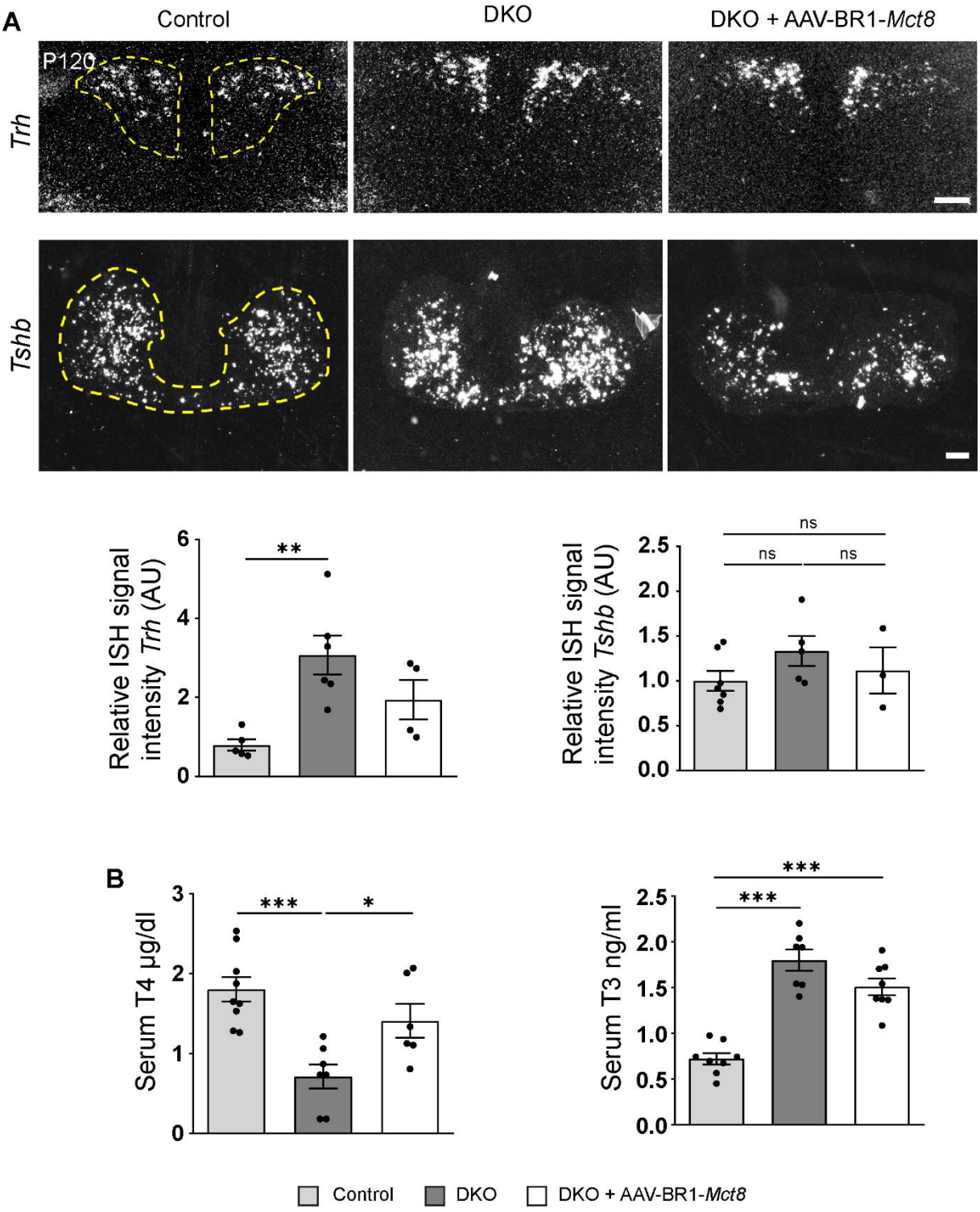

Supplementary Figure 4. AAV-BR1-*Mct8* treatment has little effect on the HPT axis.

(**A**) The expression of *Trh* and *Tshb* was detected in hypothalamic and pituitary sections of controls, DKO mice, and AAV-BR1-*Mct8*-treated DKO mice at P120 by *in situ* hybridization. AAV-BR1-*Mct8* had been administered at P0. AAV-BR1-*Mct8*-treated DKO mice showed no significant difference in *Trh* or *Tshb* expression compared to DKO mice. One-way ANOVA: *Trh*, F(2/12)=7.931, *P*=0.0064; *Tshb*, F(2/12)=1.323, *P*=0.3025; Holm-Sidak's posthoc test. Scale bar, 100 µm. (**B**) T3 and T4 concentrations in serum of P120 DKO+AAV-BR1-*Mct8*, DKO, and control mice. One-way ANOVA: T3, F(2/20)=38.09, P<0.0001; T4, F(2/20)=11.29, *P*=0.0006; Holm-Sidak's posthoc test. Each dot

represents one animal. Means ± SEM are shown. Dashed line, region of interest. ns, not significant; *, $p<0.05$; **, $p<0.01$; ***, $p<0.001$; ****, $p<0.0001$.

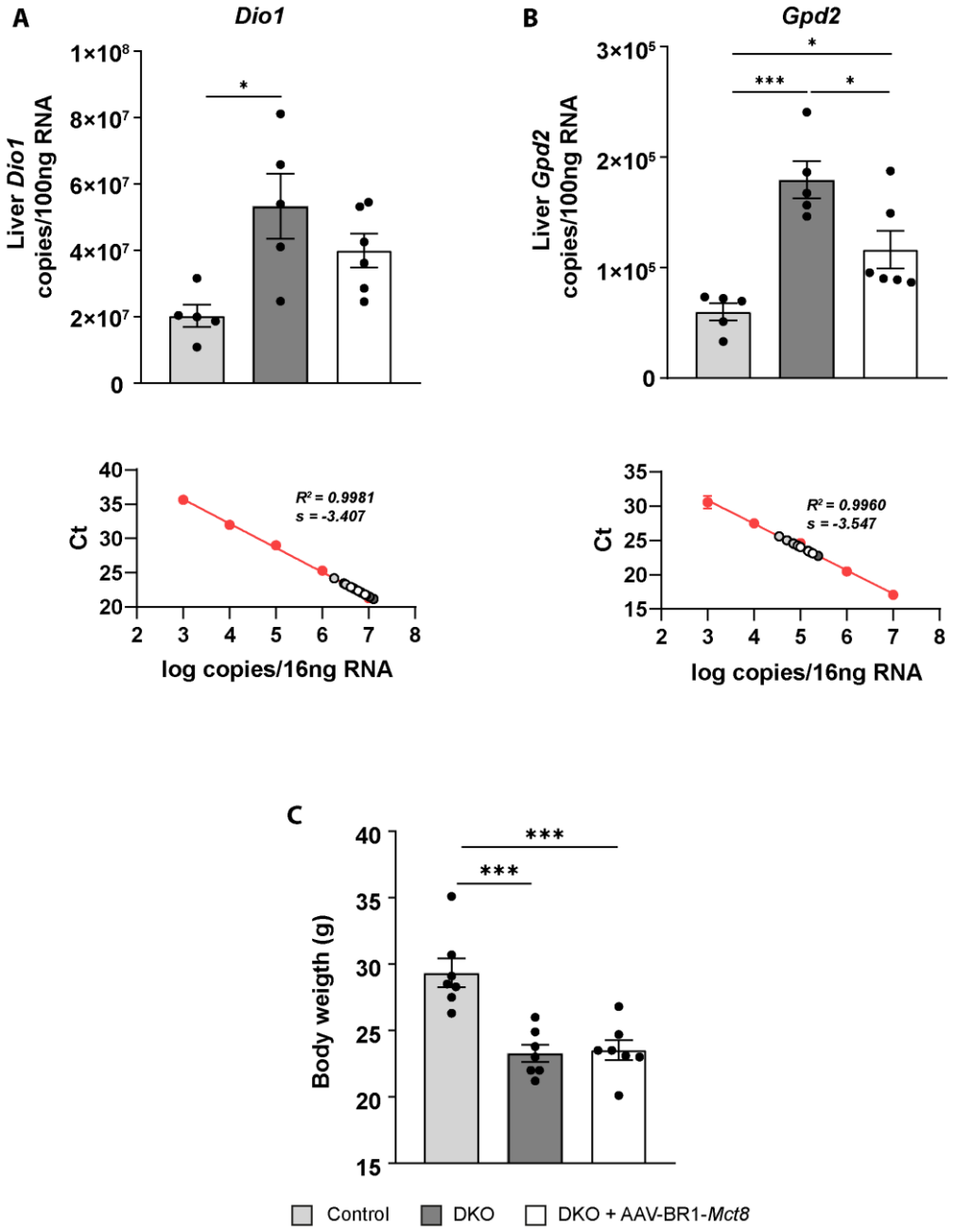

Supplementary Figure 5. AAV-BR1-*Mct8* treatment has a slight effect on peripheral hyperthyroidism of DKO mice.

(**A, B**) mRNA levels of the TH target genes *Dio1* (**A**) and *Gpd2* (**B**) in the liver of P120 controls, DKO mice, and AAV-BR1-*Mct8*-treated DKO mice. AAV-BR1-*Mct8* had been administered at P0. AAV-BR1-*Mct8* treatment did not alter the elevated *Dio1* levels. One-way ANOVA, F(2/13)=6.209, *P*=0.0128, Holm-Sidak's posthoc test. *Gpd2* was reduced by AAV-BR1-*Mct8* treatment. One-way ANOVA, F(2/13)=14.83, *P*=0.0004; Holm-Sidak's posthoc test. mRNA copies/100 ng total RNA of *Dio1* and *Gpd2* were calculated based on standard curves (Ct vs. copies) in a range of 10^3 to 10^7 copies per gene. Samples contained 16 ng total RNA per reaction. Standard curve (red) and samples are shown. (**C**) Body weight was compared among P120 controls, DKO mice, and AAV-BR1-*Mct8*-treated DKO mice. One-way ANOVA, F(2/18)=16.26, *P*<0.0001; Holm-Sidak's posthoc test. Each dot represents one animal. Means ± SEM are shown. *, *P*<0.05; ***, *P*<0.001.

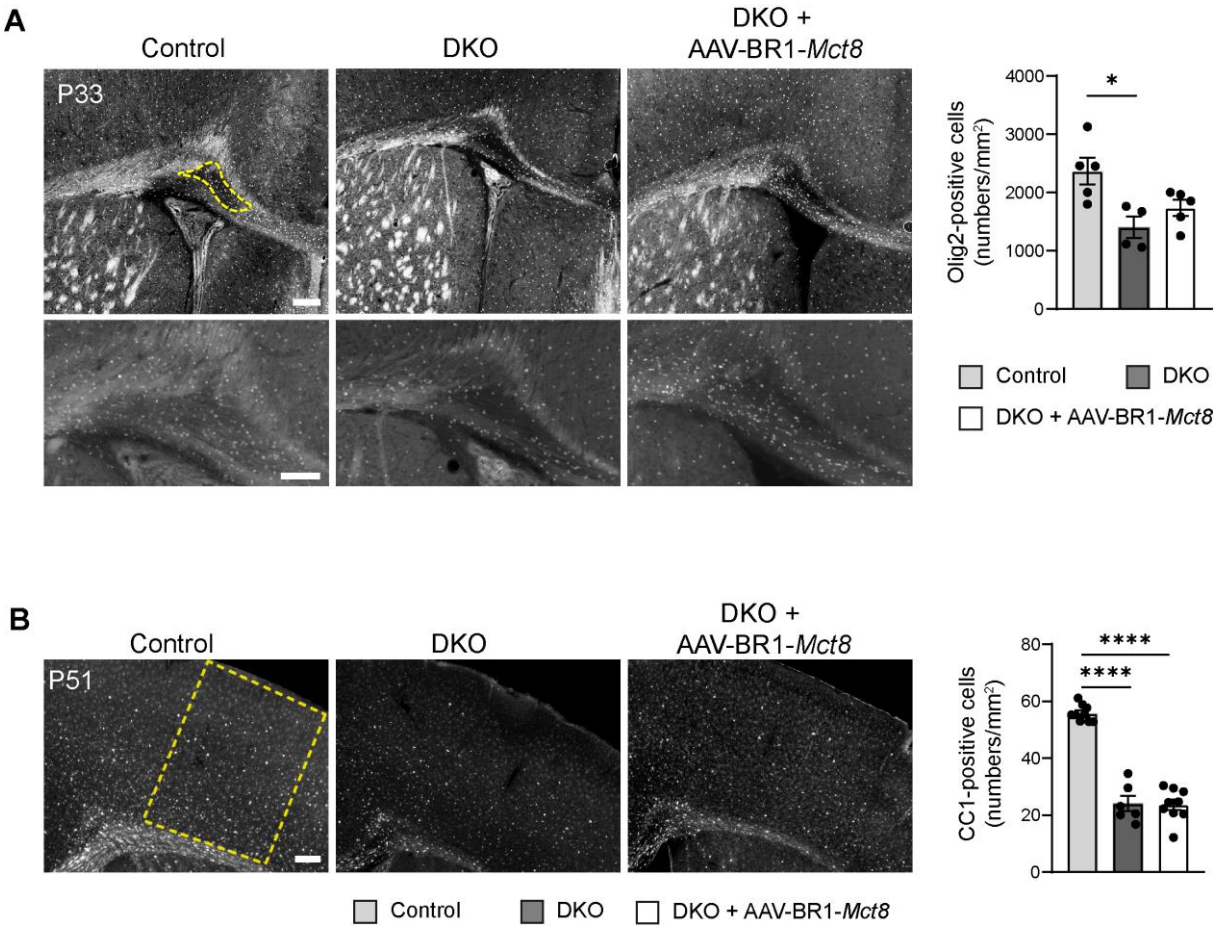

Supplementary Figure 6. Effect of AAV-BR1-*Mct8* treatment on Olig2-positive cells in corpus callosum and CC1-positive cells in cortex

(**A**) The reduced number of Olig2-immunopositive oligodendrocytes in the corpus callosum of DKO mice was slightly but nonsignificantly increased by AAV-BR1-*Mct8* treatment. AAV-BR1-*Mct8* had been administered at P0. The lower panels show a higher magnification. Scale bars, 100 µm (upper panels), 20 µm (lower panels). One-way ANOVA, $F(2/11)=6.595$, $P=0.0131$; Holm-Sidak's posthoc test. (**B**) The reduced number of mature CC1-immunopositive oligodendrocytes in the cortex of DKO mice was not significantly changed by treatment with AAV-BR1-*Mct8*. AAV-BR1-*Mct8* had been administered at P30. Scale bars, 100 µm. One-way ANOVA, $F(2/21)=110.3$, $P<0.0001$; Holm-Sidak's posthoc test. Dashed line, region of interest. *, $P<0.05$; ****, $P<0.0001$.

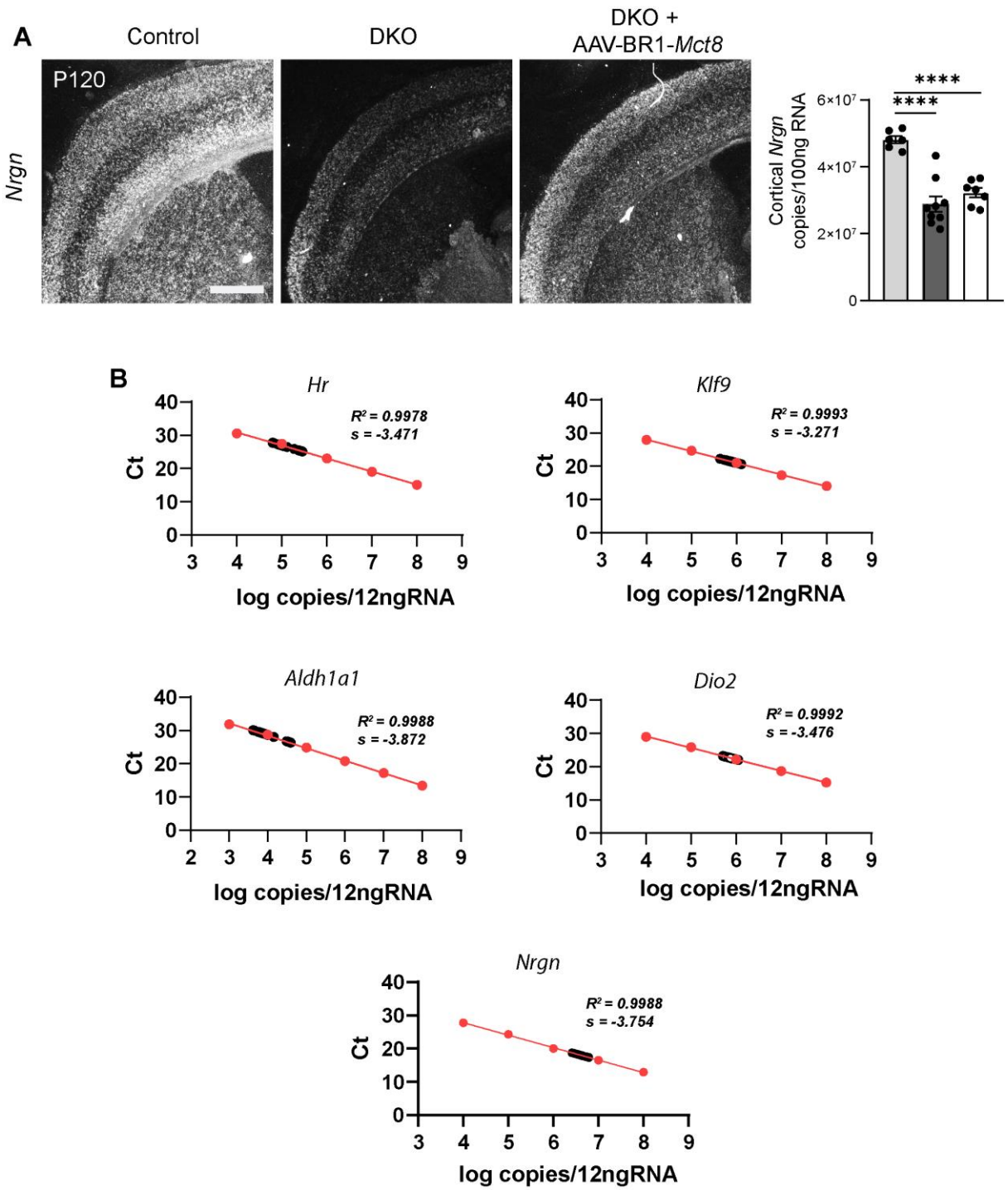

Supplementary Figure 7. Effect of AAV-BR1-*Mct8* treatment on *Nrgn* gene expression and qPCR standard curves.

(**A**) AAV-BR1-*Mct8* injected at P0 slightly but nonsignificantly increased the low expression of *Nrgn* in DKO mice at P120. Gene expression was visualised by *in situ* hybridization and quantified by qPCR. Scale bar, 100 µm. One-way ANOVA $F(2/19)=26.45$, $P<0.0001$; Holm-Sidak's posthoc test. Each dot represents one animal. Means ± SEM are shown. ****, $P<0.0001$. (**B**) Standard curves (red) and samples of **Fig. 4A-D**, **Fig. 5C** and **Supplementary Fig. 7A** (black) are shown as mRNA copies/100 ng total RNA. mRNA levels were calculated based on standard curves (Ct vs. copies) in a range of 10^3 to 10^8 copies per gene. Samples contained 12 ng total RNA per reaction.

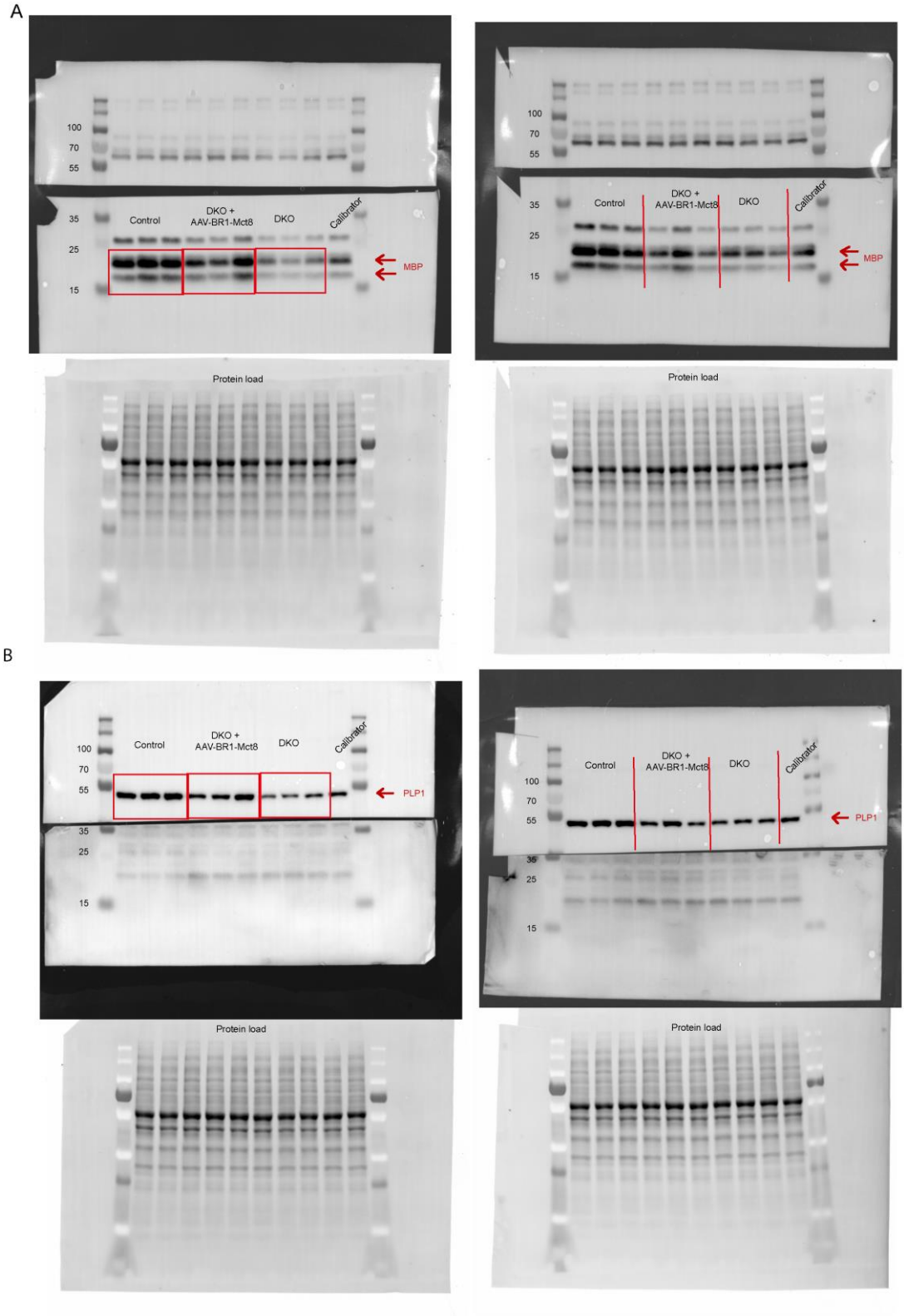

Supplementary Figure 8. Original immunoblots shown in Fig. 3

(**A**) Original blots for MBP of P21 mice and total protein load. The red boxes outline the protein bands shown in **Fig. 3A**. (**B**) Original blots for PLP1 of P21 mice and total protein load. The red boxes outline the protein bands shown in **Fig. 3B**.

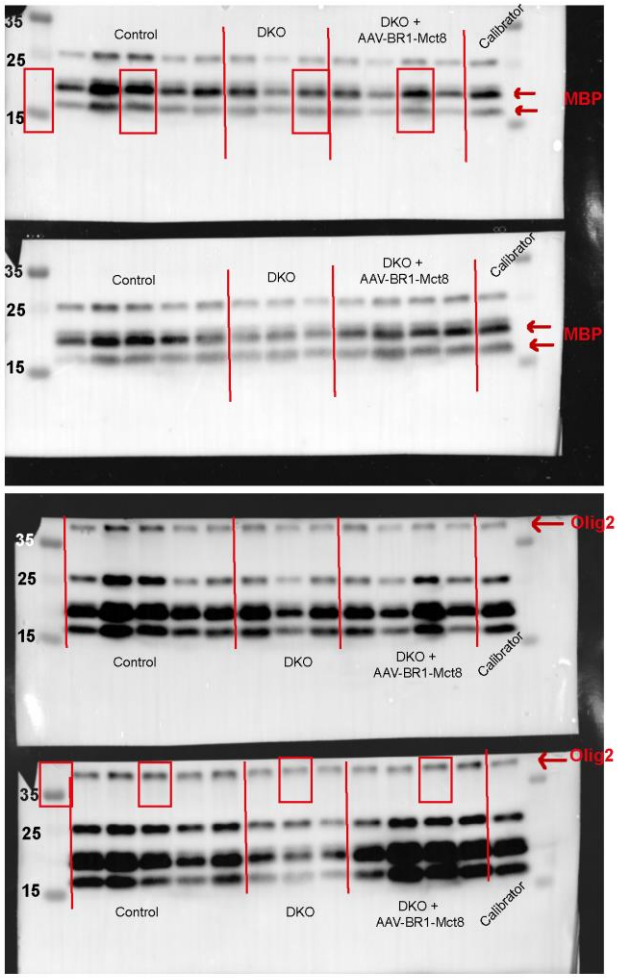

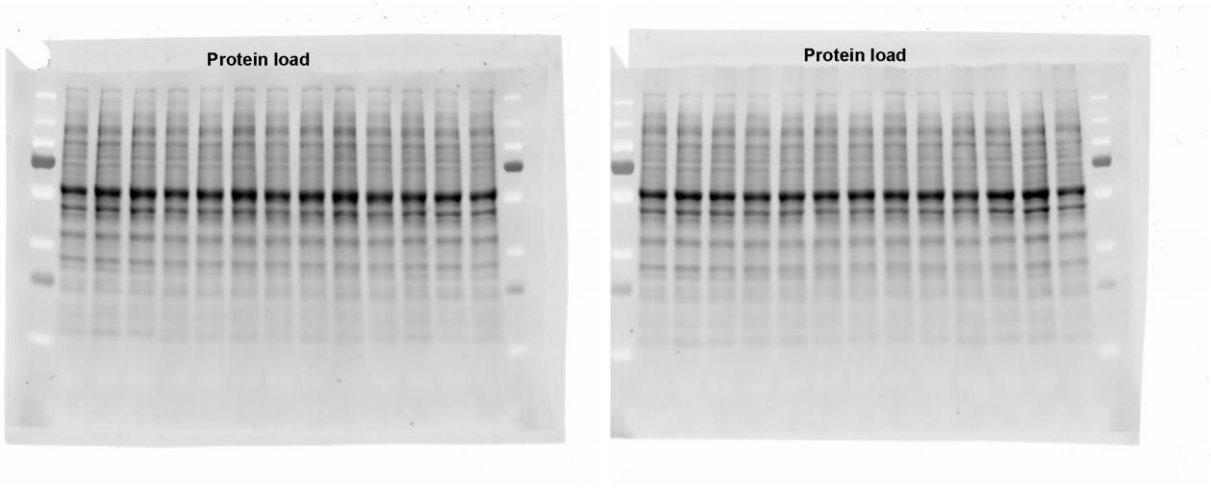

Supplementary Figure 9. Original immunoblots shown in Fig. 5

Original blots for MBP and Olig2 of P51 mice and total protein load. The red boxes outline the protein bands shown in **Fig. 5J**.

Supplementary Table 1. Sex and number of mice in the experiments.

Figure	Sex, number of mice and outliers
Fig. 1	**1C**: T3 treatment (3 ♂), AAV-BR1-*Mct8* (2 ♂), T3+AAV-BR1-*Mct8* (3 ♂), T3+AAV-BR1-*Mct8*+Silychristin (2 ♂), no outlier in any group **1E**: Control group (3 ♂), DKO (3 ♂) and DKO+AAV-BR1-*Mct8* (3 ♂) **1F**: Control group (3 ♂), DKO (3 ♂) and DKO+AAV-BR1-*Mct8* (2 ♂, 2 ♀) **1G**: Control group (5 ♂), DKO (5 ♂) and DKO+AAV-BR1-*Mct8* (5 ♂) **1H**: Control group (5 ♂), DKO (5 ♂) and DKO+AAV-BR1-*Mct8* (5 ♂) **1I**: WT group (5 ♂), Control group (5 ♂, 1 ♀), DKO (4 ♂, 2 ♀) and DKO+AAV-BR1-*Mct8* (4 ♂, 2 ♀), no outlier in any group
Fig. 2	**2A**: Molecular layer, Control group (11 ♂, 2 ♀), DKO (6 ♂, 6 ♀) and DKO+AAV-BR1-*Mct8* (7 ♂, 4 ♀) and DKO+AAV-BR1-*Gfp* (4 ♂, 2 ♀), no outlier in any group GAD67, Control group (14 ♂, 2 ♀), DKO (5♂, 6 ♀), DKO+AAV-BR1-*Mct8* (10 ♂, 4 ♀) and DKO+AAV-BR1-*Gfp* (6 ♂, 2 ♀), no outlier in any group Parvalbumin^{+} cells, Control group (9 ♂), DKO (2 ♂, 5 ♀), DKO+AAV-BR1-*Mct8* (9 ♂, 2 ♀) and DKO+AAV-BR1-*Gfp* (4 ♂, 2 ♀), no outlier in any group **2B**: Cortical thickness, Control group (3 ♂, 2 ♀), DKO (3 ♂, 2 ♀) and DKO+AAV-BR1-*Mct8* (3 ♂, 2 ♀), no outlier in any group Parvalbumin^{+} cells, Control group (4 ♂), DKO (3 ♂, 1 ♀) and DKO+AAV-BR1-*Mct8* (3 ♂, 1 ♀), no outlier in any group GAD67 intensity, Control group (4 ♂), DKO (3 ♂, 1 ♀) and DKO+AAV-BR1-*Mct8* (3 ♂, 1 ♀), no outlier in any group
Fig. 3	**3A**: Control group (3 ♂, 2 ♀), DKO (3 ♂, 3 ♀) and DKO+AAV-BR1-*Mct8* (2 ♂, 2 ♀), no outlier in any group **3B**: Control group (2 ♂, 2 ♀), DKO (2 ♂, 2 ♀) and DKO+AAV-BR1-*Mct8* (2 ♂, 2 ♀), no outlier in any group **3C**: Control group (3 ♂), DKO (3 ♂) and DKO+AAV-BR1-*Mct8* (3 ♂), no outlier in any group **3D**: Control group (5 ♂, 1 ♀), DKO (4 ♂, 2 ♀) and DKO+AAV-BR1-*Mct8* (4 ♂, 2 ♀), no outlier in any group **3E**: Control group (5 ♂, 1 ♀), DKO (4 ♂, 2 ♀) and DKO+AAV-BR1-*Mct8* (4 ♂, 2 ♀), no outlier in any group
Fig. 4	**4A**: *Hr* ISH, Control group (2 ♂+5 ♀), DKO (4 ♂, 3 ♀) and DKO+AAV-BR1-*Mct8* (2 ♂, 5 ♀) *Hr* qPCR, Control group (2 ♂, 5 ♀), DKO (6 ♂, 3 ♀) and DKO+AAV-BR1-*Mct8* (2 ♂, 5 ♀), no outlier in any group **4B**: *Klf9* ISH, Control group (2 ♂, 5 ♀), DKO (3 ♂, 3 ♀) and DKO+AAV-BR1-*Mct8* (2 ♂, 5 ♀) *Klf9* qPCR, Control group (2 ♂, 5 ♀), DKO (6 ♂, 3 ♀) and DKO+AAV-BR1-*Mct8* (2 ♂, 5 ♀), no outlier in any group **4C**: *Ald*h*1a1* ISH, Control group (2 ♂, 5 ♀), DKO (3 ♂, 3 ♀) and DKO+AAV-BR1-*Mct8* (2 ♂, 5 ♀) *Aldh1a1* qPCR, Control group (2 ♂, 5 ♀), DKO (6 ♂, 3 ♀) and DKO+AAV-BR1-*Mct8* (2 ♂, 5 ♀), no outlier in any group **4D**: *Dio2* ISH, Control group (2 ♂ + 5 ♀), DKO (3 ♂ + 3 ♀) and DKO+AAV-BR1-*Mct8* (2 ♂ + 5 ♀) *Dio2* qPCR, Control group (2 ♂, 5 ♀), DKO (6 ♂, 3 ♀) and DKO+AAV-BR1-*Mct8* (2 ♂, 1 ♀; outlier, 1 ♀) **4E**: Control group (6 ♂, 5 ♀), DKO (7 ♂, 3 ♀) and DKO+AAV-BR1-*Mct8* (5 ♂, 2 ♀), no outlier in any group **4F**: Control group (5 ♂, 4 ♀; outliers, 1 ♂, 1 ♀), DKO (4 ♂, 3 ♀; outliers,1 ♂, 1 ♀) and DKO+AAV-BR1-*Mct8* (4 ♂, 4 ♀; outlier, 1 ♀) **4G**: Control group (5 ♂, 4 ♀), DKO (4 ♂, 3 ♀) and DKO+AAV-BR1-*Mct8* (2 ♂, 3 ♀), no outlier in any group

Fig. 5	**5B**: Control group (4 ♂), DKO (3 ♂) and DKO+AAV-BR1-*Mct8* (3 ♂) **5C:** *Hr* qPCR, Control group (9 ♂, 1 ♀; outlier, 1 ♂), DKO (3 ♂, 4 ♀) and DKO+AAV-BR1-*Mct8* (5 ♂, 6 ♀) *Klf9* qPCR, Control group (10 ♂, 1 ♀), DKO (3 ♂, 4 ♀) and DKO+AAV-BR1-*Mct8* (5 ♂, 6 ♀), no outlier in any group *Aldh1a1* qPCR, Control group (10 ♂, 1 ♀), DKO (3 ♂, 4 ♀) and DKO+AAV-BR1-*Mct8* (5 ♂, 6 ♀), no outlier in any group *Dio2* qPCR, Control group (10 ♂, 1 ♀), DKO (3 ♂, 4 ♀) and DKO+AAV-BR1-*Mct8* (5 ♂, 6 ♀), no outlier in any group **5D**: Control group (9 ♂), DKO (2 ♂, 4 ♀) and DKO+AAV-BR1-*Mct8* (5 ♂, 5 ♀), no outlier in any group **5E**: Control group (8 ♂), DKO (2 ♂, 4 ♀) and DKO+AAV-BR1-*Mct8* (4 ♂, 4 ♀) no outlier in any group **5F**: Control group (7 ♂), DKO (2 ♂, 4 ♀) and DKO+AAV-BR1-*Mct8* (4 ♂, 4 ♀; outlier, 1 ♀) **5G**: Control group (9 ♂), DKO (3 ♂, 4 ♀) and DKO+AAV-BR1-*Mct8* (4 ♂, 4 ♀), no outlier in any group **5H**: Control group (9 ♂), DKO (3 ♂, 4 ♀) and DKO+AAV-BR1-*Mct8* (4 ♂, 5 ♀), no outlier in any group **5I**: Control group (9 ♂), DKO (3 ♂, 4 ♀) and DKO+AAV-BR1-*Mct8* (4 ♂, 5 ♀), no outlier in any group **5H**: Control group (9 ♂, 1 ♀), DKO (3 ♂, 3 ♀) and DKO+AAV-BR1-*Mct8* (4 ♂, 4 ♀), no outlier in any group
Suppl Fig. 1	Suppl Fig. 1A, 1B and 1C: Control group (2 ♂, 1 ♀), DKO (2 ♂, 1 ♀) and DKO+AAV-BR1-*Mct8* (2 ♂, 1 ♀), no outlier in any group
Suppl Fig. 2	Suppl Fig. 2A, 2B: Control group (2 ♂, 1 ♀), DKO (2 ♂, 1 ♀) and DKO+AAV-BR1-*Mct8* (2 ♂, 1 ♀), no outlier in any group
Suppl Fig. 3	Suppl Fig. 3C: Control group (2 ♂, 2 ♀), DKO (3 ♂, 4 ♀) and DKO+AAV-BR1-Mct8 (2 ♂, 3 ♀) Suppl Fig. 3D: Control group (2 ♂, 5 ♀), DKO (3 ♂, 5 ♀) and DKO+AAV-BR1-Mct8 (2 ♂, 3 ♀)
Suppl Fig. 4	Suppl Fig. 4A TRH: Control group (2 ♂, 3 ♀), DKO (2 ♂, 2 ♀) and DKO+AAV-BR1-*Mct8* (2 ♂, 2 ♀), no outlier in any group Suppl Fig. 4A TSH: Control group (2 ♂, 1 ♀), DKO (2 ♂, 3 ♀) and DKO+AAV-BR1-*Mct8* (2 ♂, 2 ♀), no outlier in any group Suppl Fig.4B: Control group (4 ♂, 5 ♀), DKO (4 ♂, 3 ♀) and DKO+AAV-BR1-*Mct8* (3 ♂, 5 ♀), no outlier in any group
Suppl Fig. 5	Suppl Fig. 5A and 5B: Control group (2 ♂, 3 ♀), DKO (2 ♂, 2 ♀) and DKO+AAV-BR1-*Mct8* (3 ♂, 5 ♀), no outlier in any group Suppl Fig. 5C: Control group (3 ♂, 4 ♀), DKO (4 ♂, 3 ♀) and DKO+AAV-BR1-*Mct8* (3 ♂, 4 ♀), no outlier in any group
Suppl Fig. 6	Suppl Fig. 6A: Control group (3 ♂, 2 ♀), DKO (2 ♂, 2 ♀) and DKO+AAV-BR1-*Mct8* (3 ♂, 2 ♀), no outlier in any group Suppl Fig. 6B: Control group (9 ♂), DKO (4 ♂, 2 ♀) and DKO+AAV-BR1-*Mct8* (5 ♂, 4 ♀), no outlier in any group
Suppl Fig. 7	Suppl Fig. 7A: *Nrgn* ISH, Control group (3 ♂, 2 ♀), DKO (2 ♂, 2 ♀) and DKO+AAV-BR1-*Mct8* (3 ♂, 2 ♀) *Nrgn* qPCR, Control group (2 ♂, 4 ♀; outlier, 1 ♀), DKO (6 ♂, 3 ♀) and DKO+AAV-BR1-*Mct8* (2 ♂, 5 ♀)

Supplementary references

1. Mayerl S, Muller J, Bauer R, *et al*. Transporters MCT8 and OATP1C1 maintain murine brain thyroid hormone homeostasis. *J Clin Invest*. May 2014;124(5):1987-99. doi:10.1172/JCI70324
2. Trajkovic M, Visser TJ, Mittag J, *et al*. Abnormal thyroid hormone metabolism in mice lacking the monocarboxylate transporter 8. *J Clin Invest*. Mar 2007;117(3):627-35. doi:10.1172/JCI28253
3. Urabe M, Ding C, Kotin RM. Insect cells as a factory to produce adeno-associated virus type 2 vectors. *Human gene therapy*. Nov 1 2002;13(16):1935-43. doi:10.1089/10430340260355347
4. Chen H. Intron splicing-mediated expression of AAV Rep and Cap genes and production of AAV vectors in insect cells. *Mol Ther*. May 2008;16(5):924-30. doi:10.1038/mt.2008.35

mt200835 [pii]
5. Korbelin J, Dogbevia G, Michelfelder S, *et al*. A brain microvasculature endothelial cell-specific viral vector with the potential to treat neurovascular and neurological diseases. *EMBO Molecular Medicine*. Jun 2016;8(6):609-25. doi:10.15252/emmm.201506078
6. Zolotukhin S, Byrne BJ, Mason E, *et al*. Recombinant adeno-associated virus purification using novel methods improves infectious titer and yield. *Gene Ther*. Jun 1999;6(6):973-85.
7. Wenzel J, Lampe J, Muller-Fielitz H, *et al*. The SARS-CoV-2 main protease M(pro) causes microvascular brain pathology by cleaving NEMO in brain endothelial cells. *Nat Neurosci*. Nov 2021;24(11):1522-1533. doi:10.1038/s41593-021-00926-1
8. Wilpert NM, Krueger M, Opitz R, *et al*. Spatiotemporal Changes of Cerebral Monocarboxylate Transporter 8 Expression. *Thyroid*. Sep 2020;30(9):1366-1383. doi:10.1089/thy.2019.0544
9. Heuer H, Schafer MK, O'Donnell D, Walker P, Bauer K. Expression of thyrotropin-releasing hormone receptor 2 (TRH-R2) in the central nervous system of rats. *J Comp Neurol*. Dec 11 2000;428(2):319-36.
10. De Angelis M, Giesert F, Finan B, *et al*. Determination of thyroid hormones in mouse tissues by isotope-dilution microflow liquid chromatography-mass spectrometry method. *Journal of chromatography B, Analytical technologies in the biomedical and life sciences*. Oct 15 2016;1033-1034:413-420. doi:10.1016/j.jchromb.2016.08.037
11. Müller-Fielitz H, Lau M, Jöhren O, Stellmacher F, Schwaninger M, Raasch W. Blood pressure response to angiotensin II is enhanced in obese Zucker rats and is attributed to an aldosterone-dependent mechanism. *British Journal of Pharmacology*. 2012;166(8):2417-2429. doi:10.1111/j.1476-5381.2012.01953.x
12. Oelkrug R, Krause C, Herrmann B, *et al*. Maternal Brown Fat Thermogenesis Programs Glucose Tolerance in the Male Offspring. *Cell reports*. 2020;33(5):108351. doi:10.1016/j.celrep.2020.108351
13. Assmann JC, Müller K, Wenzel J, *et al*. Isolation and Cultivation of Primary Brain Endothelial Cells from Adult Mice. *Bio Protoc*. May 20 2017;7(10)doi:10.21769/BioProtoc.2294
14. Jayarama-Naidu R, Johannes J, Meyer F, *et al*. A Nonradioactive Uptake Assay for Rapid Analysis of Thyroid Hormone Transporter Function. *Endocrinology*. Jul 2015;156(7):2739-45. doi:10.1210/en.2015-1016